PHYSICAL REVIEW A, VOLUME 62, 041802(R)

Phase-matched high-order harmonic generation in an ionized medium using a buffer gas of exploding atomic clusters

John W. G. Tisch
Laser Consortium, Blackett Laboratory, Imperial College, London SW7 2BZ, United Kingdom
(Received 10 April 2000; published 13 September 2000)

Calculations are presented of the time-dependent dispersion of a cluster medium interacting with an intense, femtosecond laser, where the clusters are ''exploding'' on the time scale of the laser pulse. It is shown that the dispersion of the clusters can transiently compensate (or buffer) the dispersion of free electrons to dramatically improve the phase matching of water-window high-order harmonic generation in the presence of strong ionization. A practical implementation of this phase-matching scheme is described.

PACS number(s): 42.65.Ky, 36.40.Vz, 42.65.Re

The nonlinear interaction of intense laser pulses with gases can result in the production of very high odd harmonics of the laser frequency, allowing coherent, short-pulse, soft-x-ray generation using short-pulse, high-power, table-top lasers. The fundamental obstacle for widespread application of this unique radiation source is the very low conversion efficiency η of laser energy into harmonic energy for the highest orders. Using sub-30-fs, mJ and sub-mJ laser pulses, high-order harmonic generation (HHG) has been demonstrated in the 2–4-nm ''water window'' with $\eta \sim 10^{-14}$/harmonic order at $\sim$2.5 nm [1,2]. A very large increase in the efficiency is required in this wavelength range to enable applications.

For maximum-efficiency HHG, the wave numbers of the harmonic field and its source, the nonlinear polarization at the harmonic frequency, must be equal. In practice, a number of factors result in a finite wave-number mismatch (or simply phase mismatch), Δk, that prevents the achievement of this phase-matched condition. To achieve very high harmonic orders, a laser intensity close to the ionization saturation intensity for the nonlinear medium must be used. Under typical experimental conditions, Δk then becomes large, dominated by the dispersion of free electrons in the interaction region. Whether or not Δk is the limiting factor in the efficiency of HHG depends on the harmonic wavelength range and the laser pulse duration. For wavelengths greater than $\sim$10 nm, and ultrafast lasers ($<$10-fs pulses), the process appears to be limited by the reabsorption of the harmonic radiation in the generating medium (i.e., absorption length is less than coherence length), as demonstrated experimentally in Ref. [3]. However, for wavelengths below 10 nm, including the important water-window range, the free-electron dephasing is viewed as the fundamental limitation to the conversion efficiency of HHG, since other known contributions to Δk that arise from focusing of the laser in the nonlinear medium [4] can, in principle, be reduced to an acceptable level by using extremely weak focusing, or by choosing a focusing geometry that minimizes these contributions [5]. This Rapid Communication is therefore focused on the free-electron problem for harmonics below 10 nm, although the other contributions to Δk are addressed.

A great deal of work has been carried out in an attempt to increase the intensity of harmonic radiation. A variety of schemes to improve the phase matching have been explored, such as quasi-phase-matching [6], high-order frequency mixing [7], and phase matching in gas-filled hollow fibers [8], but no scheme has been proposed that is applicable to harmonic wavelengths well below 10 nm, femtosecond lasers, and high free-electron densities ($>10^{18}$ cm^{-3}). A method is proposed here that is applicable to this difficult parameter regime using the dispersion of a gas of atomic clusters in a manner reminiscent of the ''buffer-gas'' method, well known to low-order nonlinear optics [9].

Atomic clusters ($\sim 10^2$–10^5 atoms) are a form of matter lying between molecules and bulk solids. Their response to strong, short-pulse laser fields has been studied extensively in recent years, both experimentally [10,11] and theoretically [12]. However, little has been published on their linear optical properties at high laser intensity, properties that are important in the understanding of short-pulse laser propagation in cluster media and the phase matching of nonlinear optical processes, such as HHG in clusters. Kim *et al.* [13] have derived an expression for the refractive index of a partially ionized cluster medium and shown theoretically that the transverse distribution in the degree of cluster ionization that occurs in a laser focus can give rise to the guiding of an intense laser pulse over a distance of more than 6 Rayleigh lengths. The present findings, concerning the potential for phase-matched HHG in a cluster medium, independently corroborate the results of the only other work that examines the optical properties of clusters at high intensity—the work of Tajima *et al.* [14]. They formulated a dispersion relation for the laser-cluster interaction, assuming *static* cluster parameters. In contrast to the present work, they did not take into account the explosion of clusters that occurs at high laser intensity that gives rise to rapidly varying cluster parameters and a hence a dispersion for the cluster medium that varies on the femtosecond time scale. The group velocity dispersion (GVD) of the cluster medium, which is not discussed by Tajima *et al.*, is also considered here.

A mixture of clusters and a collisionless monomer plasma with plasma frequency Ω_p is considered. The linear susceptibility of the mixture is $\chi = \chi_c + \chi_m$, where (in Gaussian units)

$$\chi_c = n_c \left(\frac{\varepsilon - 1}{\varepsilon + 2} \right) r^3 \tag{1}$$

is the linear susceptibility of the cluster medium [13] and

$$\chi_m = -\Omega_p^2/(4\pi\omega^2) \tag{2}$$

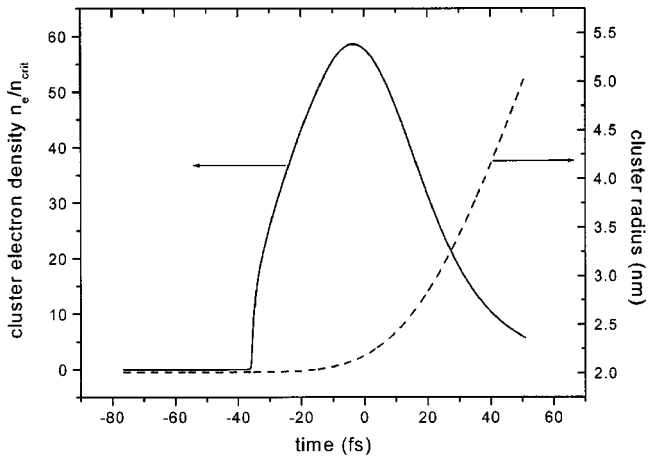

FIG. 1. Calculated time dependencies of the cluster nanoplasma electron density n_e (solid line) and radius r (dashed line) for a 2-nm-radius Ar cluster interacting with a 30-fs, 800-nm laser pulse at a peak intensity of 10^{16} W/cm^{-2}.

is the free-electron susceptibility of the monomer plasma. In Eq. (1), n_c is the density of clusters, r is the cluster radius, and ε is the dielectric function of the cluster. Assuming a nanoplasma model of the ionized cluster [12], the Drude model is used for the dielectric function:

$$\varepsilon = 1 - \frac{\omega_p^2}{\omega(\omega + i\nu)}, \tag{3}$$

where ω is the laser frequency, and ω_p and ν are the plasma frequency and the electron-ion collision frequency in the cluster nanoplasma, respectively. It is assumed that the only source of free electrons is from the monomer medium, since numerical modeling shows that the cluster electrons are largely confined to the nanoplasma in the time interval of interest here. (In the general case, a free-electron density of ΔN_e from the clusters is compensated for by reducing the monomer plasma density given below by ΔN_e.) Ignoring collisions to begin with (i.e., $\nu = 0$), substituting Eq. (3) into Eq. (1), and adding to Eq. (2) gives the complex refractive index of the mixture,

$$\eta = (1 + 4\pi\chi)^{1/2} = \left(1 - \frac{4\pi\omega_p^2 r^3 n_c}{3\omega^2 - \omega_p^2} - \frac{\Omega_p^2}{\omega^2}\right)^{1/2}, \tag{4}$$

or, in terms of the electron densities,

$$\eta = \left(1 - \frac{4\pi n_e r^3 n_c}{3n_{\rm crit} - n_e} - \frac{N_e}{n_{\rm crit}}\right)^{1/2}, \tag{5}$$

where N_e, n_e are the electron densities of the monomer plasma and the cluster nanoplasma, respectively, and $n_{\rm crit}[\mathrm{cm}^{-3}] = 3.1\times 10^{-10}(\omega[\mathrm{s}^{-1}])^2$ is the critical electron density for the laser wavelength. Only $n(\omega) = \mathrm{Re}(\eta)$ is considered, since the discussion here will be limited to cases where $N_e \ll n_{\rm crit}$ and to laser and harmonic frequencies well away from the Mie resonance at $\omega = \omega_p/\sqrt{3}$ ($n_e = 3n_{\rm crit}$).

For frequencies above the Mie resonance ($\omega > \omega_p/\sqrt{3}$), both χ_c and χ_m are negative and so $n < 1$. However, for frequencies below the resonance ($\omega < \omega_p/\sqrt{3}$), χ_c is positive while χ_m is negative, so it becomes possible to control the value of n in this frequency range to achieve phase matching, using, e.g., the monomer plasma density as the adjustable parameter. If $\omega_p/\sqrt{3}$ lies in the ultraviolet or visible range, between the laser and harmonic frequencies, then the spectral region over which n can be controlled covers near-infrared laser wavelengths (including Ti:sapphire at ~800 nm). Considering only the dispersion contribution to the phase mismatch to begin with, the general phase-matching condition for qth-order HHG is

$$\Delta k_{\rm disp} \equiv 2\pi q[n(q\omega_1) - n(\omega_1)]/\lambda_1 = 0, \tag{6}$$

where ω_1 and λ_1 are the laser frequency and vacuum wavelength, respectively. For large q, $n(q\omega_1) \approx 1$, so for the cluster/monomer mixture the phase-matching condition is

$$\frac{\Omega_p^2}{\omega_1^2} = \frac{4\pi\omega_p^2 r^3 n_c}{\omega_p^2 - 3\omega_1^2} \tag{7}$$

or, in terms of the monomer plasma density,

$$\frac{N_e}{n_{\rm crit}} = \frac{4\pi r^3 n_c (n_e/n_{\rm crit})}{n_e/n_{\rm crit} - 3}. \tag{8}$$

The inclusion of collisions ($\nu \neq 0$) does not change this condition significantly, even for the maximum expected collision frequency in the nanoplasma ($= \omega$ [12]), provided ω_1 and $q\omega_1$ are far from resonance. (However, collisions are included in the numerical dispersion model, described below.)

A practical implementation of the preceding ideas is now described. A mixture of clusters and single atoms can be produced in the gas jet from the standard type of pulsed valve used for HHG by backing the valve with a mixture of gases, one that clusters readily and one that does not. Specifically, the dispersion of a high-density medium comprising argon clusters and monomer helium is examined. This mix can be produced by backing the valve with argon at a partial pressure high enough for argon cluster formation and using the partial pressure of the helium (which does not cluster) as the control parameter. A single femtosecond laser pulse at a peak intensity of $\sim 10^{16}$ W cm^{-2} is then used both to ionize the media to create the required plasmas and to generate high-order harmonics.

During the interaction with the laser pulse, it is known that the cluster parameters r, n_e, and ν evolve on a time scale considerably shorter than the laser pulse, as the cluster plasma is heated and ionized in the laser field. Figure 1 shows the calculated time evolution of n_e (solid curve) and r (dashed curve) for a 2-nm Ar cluster interacting with a 30-fs, 800-nm laser pulse at a peak intensity of 10^{16} W cm^{-2}. Owing to the initial near solid density of the cluster, n_e reaches a value of $\sim 60 n_{\rm crit}$ near the peak of the laser pulse ($n_{\rm crit} = 1.7\times 10^{21}$ cm^{-3} at $\lambda = 800$ nm) before the cluster begins to explode. According to Eq. (8), this indicates that for realistic cluster parameters ($r \approx 2\times 10^{-7}$ cm, $n_c \approx 2\times 10^{16}$ cm^{-3}) a monomer electron density of $N_e \sim 2\times 10^{-3} n_{\rm crit}$ is required for phase matching, which is easily achieved in a gas jet. Owing to the femtosecond time evolution of the free-electron density and cluster parameters, the buffered region propagates through the nonlinear medium with the laser and har-

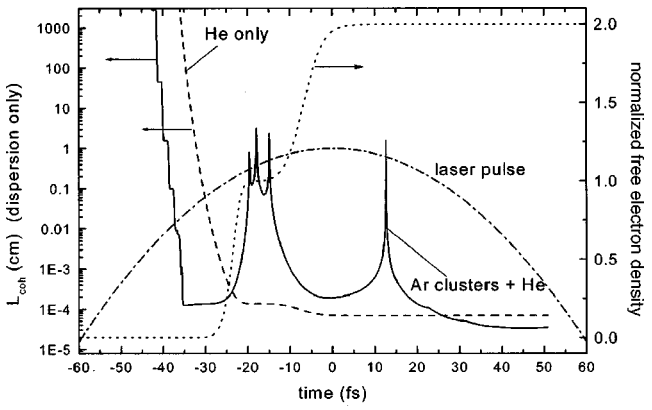

FIG. 2. Calculated coherence lengths (considering dispersion only) for the 265th harmonic generation driven by a 30-fs, 800-nm laser pulse at a peak intensity of 10^{16} W/cm^{-2}, for He alone (dashed line—refer to left axis), and for the same density of He mixed with Ar clusters (solid line—refer to left axis). The dotted line (refer to right axis) is the calculated free-electron density normalized to the initial He density. The dot-dashed line is the normalized laser intensity profile.

monic pulses. This ''traveling-wave phase matching'' is believed to be a new scheme in the context of HHG.

These time-dependent cluster calculations were performed using a numerical code based on a nanoplasma model of the laser-cluster interaction [10] which is able to reproduce accurately many experimentally observed features of the interaction [15]. This code is used to calculate $n_e(t)$, $r(t)$, and $\nu(t)$ for chosen laser pulse parameters. The calculations are repeated for a number of cluster sizes within a realistic log-normal distribution. These time-dependent data are input into a dispersion code that calculates $\eta(t)$ for the cluster/monomer mixture at any desired frequency, ω. The cluster linear susceptibility is obtained by integrating χ_c over a distribution of cluster sizes for a given preclustered atomic density. $N_e(t)$ is calculated for a chosen initial monomer (He) density (the control parameter) using tunnel-ionization rates [16]. From the dispersion of $\eta(t)$, $\Delta k(t)$ and the coherence length $L_{\mathrm{coh}}(t)=\pi/\Delta k(t)$ can be calculated for any harmonic order. The coherence length is that length over which the harmonic field grows coherently and so, for cases where it is smaller than the absorption length, sets an upper limit on the useful interaction length. The harmonic conversion efficiency, in the absence of saturation, scales as the square of L_{coh}.

Figure 2 shows the results of dispersion calculations for a 30-fs, 800-nm laser pulse at a peak intensity of 10^{16} W cm^{-2} interacting with a mixture of He atoms and Ar clusters. The He density is 3.85×10^{18} cm^{-3} (chosen to optimize the phase matching), while the density of Ar clusters is $n_c=2.25\times10^{16}$ cm^{-3} with a log-normal size distribution with a mean size of 840 atoms ($\langle r\rangle=2\times10^{-7}$ cm), which is also the half-width of the distribution [17]. The time-dependent coherence length for the harmonic $q=265$ (wavelength of 3 nm, which is in the middle of the water window) is plotted for the Ar-cluster-He mix (solid curve) and for He alone (dashed curve). Note that since only the free-electron dispersion is included, the coherence lengths are initially infinite when the electron density is zero. The dotted curve is the normalized free-electron density arising from tunnel ionization of He, while the dot-dashed curve is the laser pulse.

For He alone, $L_{\mathrm{coh}}(t)$ drops rapidly as the free-electron density increases, flattening out at a value of ~1.0 μm near the peak of the laser pulse, much shorter than the mm-scale interaction lengths available, highlighting the inefficiency of HHG in a strongly ionized medium. For the Ar-cluster–He mixture, $L_{\mathrm{coh}}(t)$ exhibits two main peaks where the phase matching is dramatically improved owing to the buffering action of the clusters. To ensure a relatively uniform free-electron density distribution in the focus (in r and z) directions, the experimental parameters were chosen to synchronize the first phase-matching peak with the saturation of He^+ ionization that occurs at $\sim5\times10^{15}$ W cm^{-2} at $t\approx-15$ fs. This increases the volume of the region where the phase matching is improved (the cluster explosion dynamics are relatively insensitive to intensity above $\sim10^{15}$ W cm^{-2} [15]). The second phase-matching peak occurs after the saturation of He^+ ionization (i.e., fully stripped He), and is thus of no interest here. Three very narrow ($<$1-fs duration) subpeaks are visible where $L_{\mathrm{coh}}(t)$ reaches a maximum value of several cm. Averaging over these, the width of the peak is ~5 fs with a peak coherence length of ~1 mm, comparable to the maximum high-density interaction length possible in a standard gas jet. During this peak, generation of the 265th harmonic from the clusters and the He^+ ions is phase-matched over the interaction length, provided there is negligible group-velocity walkoff between the laser and harmonic pulses, which is a requirement of traveling-wave phase matching. While HHG has been observed in cluster media, attention is focused on HHG from He^+ ions. He^+ has a predicted cutoff [18] at around $q=645$ (1-keV harmonic photons) for an intensity of 5×10^{15} W cm^{-2}, so $q=265$ would be in the plateau of the He^+ harmonic spectrum. For a given intensity the ion polarizability is lower than for the atom; however, the ionic dipole can be driven much harder before ionizing, so the maximum dipole emission strength is expected to be comparable to neutral He, but extended to higher orders [19]. By buffering the interaction with clusters, it thus seems that the previously intractable problem of free-electron dispersion may be overcome, and the potential of ions for high-order HHG realized.

Figure 3 shows the dispersion curve (refractive index versus vacuum wavelength) for the Ar-cluster–He mix during the phase-matching peak (solid curve), showing that the refractive index at the laser wavelength is near unity as required for phase matching the high-order harmonics ($q>\sim101$). The dashed line shows the strong free-electron dispersion of the He^+ plasma without the clusters, while the dotted line represents the dispersion of the Ar clusters in the absence of the He^+ plasma. GVD calculations for the buffered case indicate that there is only a small amount of group-velocity walkoff between the laser and harmonic pulses (~5 fs over a 1-mm interaction length) and negligible GVD broadening of the laser pulse ($<$0.1 fs).

The other contributions to Δk arising from the focusing of the laser are now considered, namely, those from the Gouy phase of the laser, Δk_{Gouy}, and from the intensity-dependent

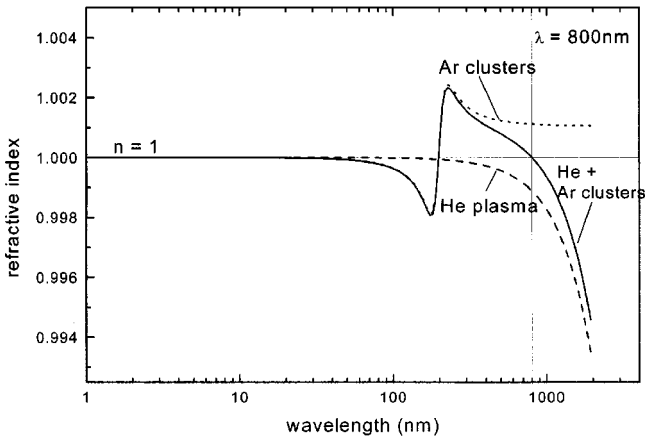

FIG. 3. Calculated dispersion during the phase-matching peak occurring at −15 fs (see Fig. 2) for the Ar-cluster–He mix (solid line), for the Ar clusters alone (dotted line), and for the He plasma alone (dashed line).

dipole phase, $\Delta k_{\mathrm{dipole}}$ [20]. Δk_{Gouy} has the same sign as Δk_{disp} (i.e., positive) and is much smaller than Δk_{disp} for the parameter values considered here, and so it can be buffered by the cluster dispersion, provided it has an approximately constant value along the interaction length (z axis). This condition is met if the laser waist is centered in the nonlinear medium (of length L) and $b > \sim 5L$, where b is the laser confocal parameter. Then, the maximum Gouy phase mismatch is $\Delta k_{\mathrm{Gouy}} \approx 2q/b \approx 34\pi/\mathrm{mm}$ for $q=265$ and $b=5$ mm (corresponding to a diffraction-limited Gaussian focal spot radius $w_0 = 25\ \mu$m at $\lambda_1 = 800$ nm, so ~3 mJ of laser energy in a 30-fs pulse are required for a peak intensity of 10^{16} W cm^{-2}) compared to $\Delta k_{\mathrm{disp}} \approx 730\pi/\mathrm{mm}$ for the unbuffered case above. As expected, phase-matching simulations with $\Delta k = \Delta k_{\mathrm{disp}} + \Delta k_{\mathrm{Gouy}}$ show an identical phase-matching peak to Fig. 2 at a slightly reduced He density of 3.69×10^{18} cm^{-3}. $\Delta k_{\mathrm{dipole}}$ is more difficult to quantify, since calculations for ions at intensities around 10^{16} W cm^{-2} have not been made. But extrapolating exist-ing data [21] to higher intensity suggests a linear dependence of the dipole phase with laser intensity I according to $\varphi[\mathrm{rad}] \approx -2 \times 10^{-13} I$ [W/cm^{-2}]. Therefore, from the z dependence of I for a Gaussian focus, in the loose-focusing limit, $\Delta k_{\mathrm{dipole}}$ has a value that varies along the interaction length according to $\Delta k_{\mathrm{dipole}} \approx 8\varphi z/b^2$ (essentially independent of q), and so cannot be buffered effectively using the cluster dispersion. However, for $b=5$ mm and $I = 5 \times 10^{15}$ W cm^{-2}, the corresponding coherence length [defined as $\int_0^{L_{\mathrm{coh}}^{\mathrm{dipole}}} \Delta k_{\mathrm{dipole}}(z)dz = \pi$] is $L_{\mathrm{coh}}^{\mathrm{dipole}} \approx 140\ \mu$m. This is considerably smaller than the buffered coherence length above (≈1 mm) in the absence of $\Delta k_{\mathrm{dipole}}$, but the overall coherence length is still ~120× the unbuffered value. Obviously, $\Delta k_{\mathrm{dipole}}$ could be reduced by using focusing looser than $b=5$ mm, laser energy permitting.

In conclusion, these are, to our knowledge, the first calculations of the time-dependent dispersion of a cluster medium at high laser intensity in which the individual clusters are exploding on the time scale of the femtosecond laser pulse. The time dependencies of the cluster parameters that enter into the dispersion calculations are obtained from a tested numerical nanoplasma code. The results of these dispersion calculations predict that for an intense, femtosecond laser pulse interacting with a mixture of a monomer and a cluster medium (with a realistic cluster-size distribution), the dispersion of the free electrons (and the Gouy phase mismatch in most cases) can be transiently compensated in certain spectral ranges by the dispersion of the cluster nanoplasmas. Calculations were presented for a mix of Ar clusters and He, showing a large increase (factor of $\sim 10^4$) in the coherence length for a water-window harmonic compared to the unbuffered case. For the extended, high-density interaction lengths made possible, reabsorption of the harmonic radiation in the cluster medium may become the limiting factor. Cluster plasma x-ray absorption calculations are a topic for future work.

The author was financially supported by EPSRC. Assistance with the nanoplasma simulations from E. Springate and fruitful discussions with J. P. Marangos, R. A. Smith, and M. H. R. Hutchinson are gratefully acknowledged.

[1] Z. Chang *et al.*, Phys. Rev. Lett. **79**, 2967 (1997).
[2] M. Schnürer *et al.*, Phys. Rev. Lett. **80**, 3236 (1998).
[3] M. Schnürer *et al.*, Phys. Rev. Lett. **83**, 722 (1999).
[4] See, e.g., P. Balcou *et al.*, Phys. Rev. A **55**, 3204 (1999).
[5] P. Salières, A. L'Huillier, and M. Lewenstein, Phys. Rev. Lett. **74**, 3776 (1995).
[6] P. L. Shkolnikov, A. Lago, and A. E. Kaplan, Phys. Rev. A **50**, R4461 (1994).
[7] P. L. Shkolnikov, A. E. Kaplan, and A. Lago, Opt. Lett. **18**, 1700 (1993).
[8] C. G. Durfee III *et al.*, Phys. Rev. Lett. **83**, 2187 (1999).
[9] See, e.g., J. F. Reintjes, *Nonlinear Optical Parametric Processes in Liquids and Gases* (Academic Press, Orlando, 1984), pp. 49–52.
[10] T. Ditmire *et al.*, Phys. Rev. A **57**, 369 (1997).
[11] M. Lezius *et al.*, Phys. Rev. Lett. **80**, 261 (1998).
[12] T. Ditmire *et al.*, Phys. Rev. A **53**, 3379 (1996).
[13] A. V. Kim *et al.* in *Superstrong Fields in Plasmas*, edited by M. Lontano, G. Mourou, F. Pegoraro, and E. Sindoni, AIP Conf. Proc. No. 426 (AIP, Woodbury, NY, 1998), pp. 79–84.
[14] T. Tajima, Y. Kishimoto, and M. C. Downer, Phys. Plasmas **6**, 3759 (1999).
[15] E. Springate *et al.*, Phys. Rev. A **61**, 063201 (2000).
[16] M. Ammosov, N. Delone, and V. Krainov, Sov. Phys. JETP **64**, 1191 (1986).
[17] M. Lewerenz, B. Schilling, and J. P. Toennies, Chem. Phys. Lett. **206**, 381 (1993).
[18] J. L. Krause *et al.*, Phys. Rev. Lett. **68**, 3535 (1992).
[19] J. L. Krause, K. J. Schafer, and K. C. Kulander, Phys. Rev. Lett. **68**, 3535 (1992).
[20] M. Lewenstein, P. Salières, and A. L'Huillier, Phys. Rev. A **52**, 4747 (1995).
[21] A. L'Huillier and C. G. Wahlström (private communication).